Available online at www.sciencedirect.com

ScienceDirect

Current Opinion in Electrochemistry

Review Article

Recent advances in nanoelectrochemistry at the interface between two immiscible electrolyte solutions

Conrad Benjamin Milton[1], Kerui Xu[1] and Mei Shen[1,2]

Abstract

The nanoscale interface between two immiscible electrolyte solutions (nanoITIES) is an emerging versatile analytical platform. Analytical advantages of chemical analysis using the nanoITIES include imaging with nanometer spatial resolution, probing fast dynamics with millisecond temporal resolution and fast response times, selectively detecting analytes, probing fundamental chemical processes (e.g., diffusion profiles), and versatile sensing of metal ions, proteins, neurotransmitters, ionic and neutral species, redox-active and non-redox active analytes, etc. We present here a brief theoretical background of the nanoITIES and experimental advances from the past five years. These advances include imaging of nanopores, probing diffusion profiles, biosensing, a new pH modulation mechanism for sensing neutral species, and studying exocytosis from *Aplysia californica* neurons.

Addresses

[1] Department of Chemistry, University of Illinois at Urbana-Champaign, 600 S Mathews Ave, Urbana, IL 61801, United States

[2] The Beckman Institute for Advanced Science and Technology, University of Illinois at Urbana-Champaign, 405 N Mathews Ave, Urbana, IL 61801, United States

Corresponding author: Shen, Mei (mshen233@illinois.edu)

Current Opinion in Electrochemistry 2022, **34**:101005

This review comes from a themed issue on **Physical & Nano-Electrochemistry (2022)**

Edited by **Taek Dong Chung**

For complete overview about the section, refer Physical & Nano-Electrochemistry (2022)

Available online 6 April 2022

https://doi.org/10.1016/j.coelec.2022.101005

Keywords

Interface between two immiscible electrolyte solutions, NanoITIES, Nanoimaging, Exocytosis, Neurotransmitter sensing, Biosensing, Nanopore arrays.

Introduction

The interface between two immiscible electrolyte solutions (ITIES) has been demonstrated as a versatile analytical platform to detect metal ions [1–4], proteins [5], and neurotransmitters [6–14]. The ITIES is typically formed between two solvents with low mutual miscibility where one phase is aqueous and the other phase is a polar organic solvent that has a moderate to high dielectric permittivity [15]. Compared to conventional solid electrodes (e.g., carbon, platinum), ITIES has the benefit of being able to detect non-redox active species without the enzymatic modifications often needed when using solid electrodes [16]. Thus, ITIES platforms expand the capability of electrochemistry to detect both redox-active and non-redox active analytes, where the detection is based on one type of faradaic processes-ion transfer [9,16–21], in contrast to the electron transfer that commonly occurs at a solid electrode/solution interface. This ion transfer across the ITIES was described by the Marcus theory, which proposed that an ion undergoes initial desolvation from the first phase accompanied by concerted solvation into the second phase [22].

The field of ITIES has several decades of history, with the whole field advancing from the macroITIES to the microITIES and then to the nanoITIES. Here, we mainly discuss developments at the nanoITIES from 2017 until now. The works presented here are not possible without earlier pioneering work, however, due to space limitations, we refer the readers to other publications about the macroITIES, microITIES, and early nanoITIES [1–4,8,9,23–55]. Nanoscale electrodes have analytical advantages of faster diffusive mass transport, low background interference due to the small capacitive current of nanoscale electrodes [16], and improved spatial resolution [16,45,56,57]. In addition, nanoITIES electrodes are not subject to electrostatic damage as has been reported for metal nanoelectrodes [58]. These advantages contributed to the miniaturization of supporting structures for the ITIES to the nanoscale [45]. The nanoITIES has been supported by both nanopore arrays and nanopipettes for the purpose of ionic sensing, nanoscopic imaging, characterization of diffusion [59–62], and studying cellular release mechanisms [63,64] at the nanoscale.

We begin this article by discussing the working principles (e.g., thermodynamics) of ion transfer across the ITIES. We then describe the electric double layer at the ITIES and methods for characterizing nanopipettes for the nanoITIES. Finally, we discuss recent studies that used the nanoITIES to characterize diffusion at nanopore arrays, model drug transfer across hydrophobic bacterial membranes, and detect

neurotransmitters to enable exciting cellular studies. We hope these recent advances will stimulate further discoveries in nanoscience, chemistry, neuroscience, and biomedicine.

Working principles of nanoITIES

Kinetics and thermodynamics of ion transfer at ITIES are analogous to electron transfer at solid electrode/solution interface. The determination of kinetic parameters (e.g., standard rate constant and transfer coefficient) at the ITIES can be achieved based on Butler-Volmer equation [48,65,66]. Advantages of faster mass transport at nanoITIES allow the measurement of fast ion transfer kinetics at the nanoITIES. Amemiya, Mirkin and colleagues developed a new method for kinetic analysis at the nanoITIES [48]. As with electron transfer at the solid electrode/solution interface, an ion's electrochemical potential is the same in the initial and final phases of the transfer at equilibrium. Deriving from the electrochemical potential, for the transfer of ion M^z from the water (w) to oil (o) phase, the Galvani potential difference ($\Delta^o_w\phi$) is expressed as:

$$\Delta^o_w\phi = \left(\mu^{0,w}_{M^z} - \mu^{0,o}_{M^z}\right) \Big/ zF + (RT/zF)\ln\left(\alpha^w_{M^z}/\alpha^o_{M^z}\right)$$

$$\Delta^o_w\phi = \Delta^o_w\phi^0_{M^z} + (RT/zF)\ln\left(\alpha^w_{M^z}/\alpha^o_{M^z}\right) \quad (1)$$

In Equation (1), $\mu^{0,p}_{M^z}$ is the standard chemical potential of ion M^z in phase p (w or o), z is the charge on ion M, F is Faraday's constant, R is the ideal gas constant, T is the temperature, $\alpha^p_{M^z}$ is the activity of ion M^z in phase p, and $\Delta^o_w\phi^0_{M^z}$ is the standard Galvani potential difference of transferring ion M^z from w to o, which is:

$$\Delta^o_w\phi^0_{M^z} = \left(\mu^{0,w}_{M^z} - \mu^{0,o}_{M^z}\right)\Big/zF = -\Delta G^{0,w\to o}_{tr}\Big/zF \quad (2)$$

In Equation (2), $\Delta G^{0,\ w\to o}_{tr}$ is the standard free energy needed to transfer ion M^z from w to o. $\Delta^o_w\phi^0_{M^z}$ is specific to different analytes being transferred across an ITIES, allowing for differentiation and selective detection of analytes. In addition, ion-transfer assisting ionophores [67] and/or different oil phase solvents modulate the analyte's $\Delta^o_w\phi^0_{M^z}$ [12,29,66,68].

The diffusion-limited current (i) of a single-channel micro- and nano-pipette with a disc geometry is related to the radius of the ITIES according to the expression [69]:

$$i = 4xnFcDa \quad (3)$$

In Equation (3), x is a function related to the quantity $RG = r_g/a$ [46], where r_g and a are the outer and inner tip radii, respectively, n is the number of charges transferred across the nanoITIES per analyte ion, F is Faraday's constant, c is the concentration of the ionic analyte, and D is the diffusion coefficient of the ionic analyte. Solving Equation (3) for a allows the electrode's inner radius to be calculated from electrochemical data. For ITIES arrays where all the ITIES within the array are diffusionally independent, the diffusion-limited ion-transfer current is described by a different equation (Equation (4))

$$i = N_p 4nFDca \quad (4)$$

where N_p is the number of pores in the array that forms the ITIES [36] while the rest of parameters are defined above.

Electric double layer at ITIES

Non-faradaic processes (no charge transfer) and faradaic processes (charge transfer) occurring at an ITIES resemble those at solid electrodes (e.g., carbon, platinum). An electrode at which no charge transfer can occur across the electrode/solution interface is called an ideal polarizable electrode (IPE) [66]. Since charge cannot transfer across the IPE interface when the potential is changed, the electrode/solution interface behaves like a capacitor so that charge accumulates on the metal electrode and in the solution until $q = C \times E$. q, E, and C are the charge stored on the capacitor, the potential across the capacitor, and the capacitance, respectively [66]. The whole array of charged species and oriented dipoles existing at the metal-solution interface is called *the electric double layer* [66]. The solution side of the double layer is thought to be made up of several "layers," including an inner layer (containing solvent molecules and specifically adsorbed species) and a "diffuse" layer (composed of nonspecifically adsorbed solvated ions, which extends from the outer Helmholtz plane (OHP) into the bulk of the solution) [66]. The OHP is the locus of the center of the nearest solvated ions [66].

The ITIES double layer is analogous to that at the metal-solution interface with new studies carried out to uncover new phenomena regarding double layer structure at the ITIES [70–79]. In 1939, Verwey and Niessen described the electric double layer at the ITIES as two non-interacting "diffuse" layers, one at each side of the interface. It is unclear if this "diffuse" layer has the same composition as the one described above. They stated that, for the ITIES, every electrolyte added to the system is potential determining. The electrolyte is generally distributed unequally about both phases and builds up an electric double layer at the ITIES as a consequence of the generally unequal distribution

coefficients of the positive and negative ions [80]. Later, Verwey described that since there are no space charges involved in the bulk aqueous phases, the ionic concentrations remain constant. Therefore, when approaching the region near the interface, the ionic concentration of one sign increases and the other sign decreases, ensuring a balance of the total charge for both phases with opposite signs [81]. In 1988, Marecek, Samec and Koryta published a detailed review article regarding charge transfer across the ITIES, where the theory of

Figure 1

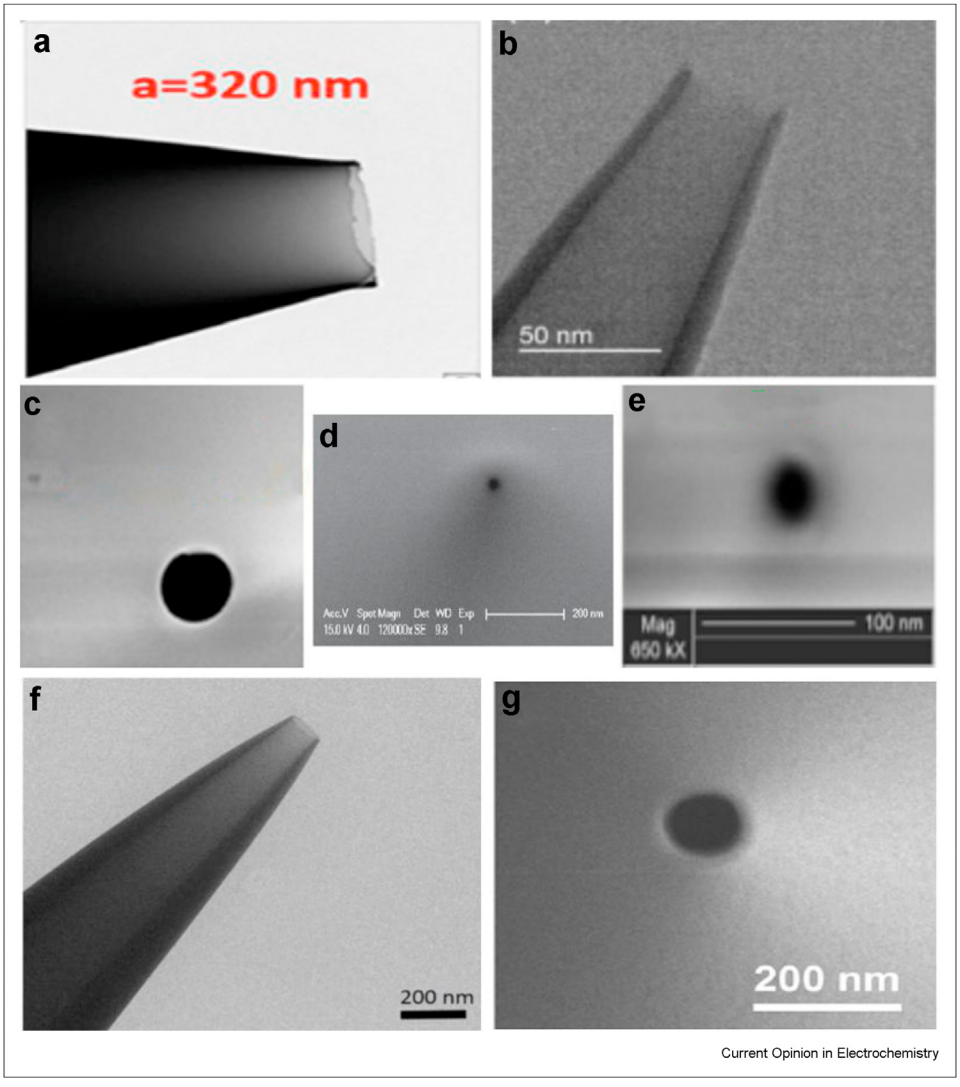

Characterization of quartz glass nanopipettes for nanoITIES using SEM and TEM. **(a)** A TEM image of a nanopipet tip of inner radius 320 nm. Reprinted with permission from N.T. Iwai, M. Kramaric, D. Crabbe, Y. Wei, R. Chen, M. Shen, GABA Detection with Nano-ITIES Pipet Electrode: A New Mechanism, Water/DCE-Octanoic Acid Interface, Anal. Chem. 90 (2018) 3067–3072. Copyright 2018 American Chemical Society. **(b)** A TEM image of a quartz nanopipette at × 100,000, with an inner diameter of ~30 nm. Reprinted with permission from R. Chen, R.J. Balla, A. Lima, S. Amemiya, Characterization of Nanopipet-Supported ITIES Tips for Scanning Electrochemical Microscopy of Single Solid-State Nanopores, Anal. Chem. 89 (2017) 9946–9952. Copyright 2017 American Chemical Society. **(c)** A SEM image of a nanopipet tip of inner radius 340 nm. Reprinted with permission from N.T. Iwai, M. Kramaric, D. Crabbe, Y. Wei, R. Chen, M. Shen, GABA Detection with Nano-ITIES Pipet Electrode: A New Mechanism, Water/DCE-Octanoic Acid Interface, Anal. Chem. 90 (2018) 3067–3072. Copyright 2018 American Chemical Society. **(d)** A SEM image of a nanopipet tip of ~15 nm inner radius. Reprinted with permission from M. Shen, R. Ishimatsu, J. Kim, S. Amemiya, Quantitative imaging of ion transport through single nanopores by high-resolution scanning electrochemical microscopy, J. Am. Chem. Soc. 134 (2012) 9856–9859. Copyright 2012 American Chemical Society. **(e)** A SEM image of a nanopipette with a radius of ~15 nm. Reprinted with permission from M.L. Colombo, J. V Sweedler, M. Shen, Nanopipet-based liquid–liquid interface probes for the electrochemical detection of acetylcholine, tryptamine, and serotonin via ionic transfer, Anal. Chem. 87 (2015) 5095–5100. Copyright 2015 American Chemical Society. **(f)** A TEM image of a nanopipette of orifice radius 76 nm. Reprinted with permission from M. Zhou, Y. Yu, P.-Y. Blanchard, M. V Mirkin, Surface Patterning Using Diazonium Ink Filled Nanopipette, Anal. Chem. 87 (2015) 10956–10962. Copyright 2015 American Chemical Society. **(g)** A SEM image of a nanopipet. Reprinted with permission from S.R. Puri, J. Kim, Kinetics of Antimicrobial Drug Ion Transfer at a Water/Oil Interface Studied by Nanopipet Voltammetry, Anal. Chem. 91 (2019) 1873–1879. Copyright 2019 American Chemical Society.

the electric double layer was further described [49]. In 2020, Girault and colleagues showed that at the ITIES, the potential difference takes place between two closely interacting ionic monolayers, where ions of opposite charges directly neutralize each other leading to an absence of diffuse layers and charge screening by surrounding ions [78]. The effect of the adsorption of charged species on the charge distribution at the ITIES was also simulated based on the description of the interface employing the Gouy-Chapman model [76–79]. Overall, the structure of the double layer at the ITIES is still an active area of research. The nanoITIES has a small electric double layer charging current due to the nanoscale size of the electrodes, producing a low background current that enables high signal to noise ratio measurements.

Characterization of Nanopipettes for nanoITIES

Protocols have been developed for fabricating nanopipettes for nanoITIES studies in a reproducible and easy to fabricate manner [8–10,12,26,47,56,82,83]. The electrochemical response of nanopipettes is significantly affected by the physical geometry and surface chemistry of the pipettes, particularly at the tip [84,85]. The geometry of pipettes can be inspected using several electron microscopy techniques as shown in Figure 1, including scanning electron microscopy (SEM), scanning transmission electron microscopy (STEM), and transmission electron microscopy (TEM) [9,10,47,61,86–89]. The inner radius (r_i), outer radius (r_g), and cone angle (θ) are the three crucial parameters that define pipette geometry [90,91]. Besides microscopic techniques, the sizes of the nanopipettes can also be determined using Equation (3) for an ITIES of disc geometry by measuring the diffusion-limited transfer current of an ion with a known diffusion coefficient and concentration, such as tetrabutylammonium (TBA) [40,47]. In addition, the solid angle method [37], electrochemical resistance method [92,93], and SECM method [94] have been reported to characterize nanopipettes. Another nanopipette characterization method uses SECM approach curves, where a simulated approach curve generated using electrochemical theory is fitted to experimental data. This simulation allows for determination of geometrical features of the nanopipette, such as r_i, r_g, and the amount of recession for the electroactive interface [29,94].

Application of the ITIES to study nanopore arrays

Two kinds of studies have been reported related to nanopore arrays including 1) nano-imaging of a nanopore array using a nanoITIES tip, and 2) studying the diffusion profile of nanopore arrays via an ITIES reaction in the arrays (i.e., silica deposition or tetrapropylammonium ion transfer).

In 2012, Shen et al. demonstrated the nanoITIES as a powerful analytical platform to image a nanopore array coupled with scanning electrochemical microscopy (SECM) [47]. In this study, nanometer resolution was achieved and the pore spacing of a nanopore array was clearly visualized. More recently, Chen et al. demonstrated that protruded nanoITIES tips were able to be used for SECM characterization of nanopore arrays. The authors successfully imaged individual nanopores with nanometer spatial resolution using a protruded nanoITIES. Finite element simulations showed that the SECM imaging with a protruded nanoITIES gave enlarged sizes of the nanopores. However, the enlarged nanopore sizes did not affect the spatial resolution of the SECM nanopore imaging (Figures 2a and b) [61].

The ITIES was also used to determine the diffusion characteristics across a nanopore array and the location of the ITIES in the nanopores [59,60]. In 2016, Liu et al. probed overlapped diffusion and independent diffusion at nanopore arrays via electrochemically assisted formation of silica deposits based on ion transfer across a nanoITIES [60]. In 2018, Holzinger et al. used this silica deposition strategy with FIB/SEM tomography to further probe diffusion across nanopore arrays [59]. Figure 2c shows the different orientations of nanopores, both front- and back-side milled, that were used. Figure 2d shows a two-dimensional SEM image of the silica residues deposited around the nanopores. By stacking these images on each other, a three-dimensional reconstruction of the silica deposition was nicely created (Figure 2e) [59]. In addition to these square nanopore arrays, hexagonal nanopore arrays were characterized as supports for the nanoITIES by a recent study where it was demonstrated that the ion-transfer behaviors at nanoITIES arrays are not only dependent on the ratio of the center-to-center distance (r_c) to the nanopore radius (r_a) (r_c/r_a), but also influenced by the design features of the nanoarrays that form the interfaces. For example, a r_c/r_a of at least 96 was needed for independent diffusion across the hexagonal nanopores to occur, while a r_c/r_a of only 56 was sufficient for independent diffusion to occur in square nanopore arrays [62].

Application of the nanoITIES to detecting biologically relevant species

Detection and quantitation of charged and uncharged neurotransmitters has been reported using nanoITIES electrodes [8–10,12–14]. Iwai et al. demonstrated detection of a neutral analyte (i.e., the zwitterion γ-aminobutyric acid (GABA)) at the nanoITIES by introducing a novel detection mechanism involving pH modulation. Specifically, the pH of the oil phase was decreased with an organic acid to protonate GABA to its cationic form upon detection at the ITIES (Figure 3a). The cationic form of GABA binds to the ionophore

Figure 2

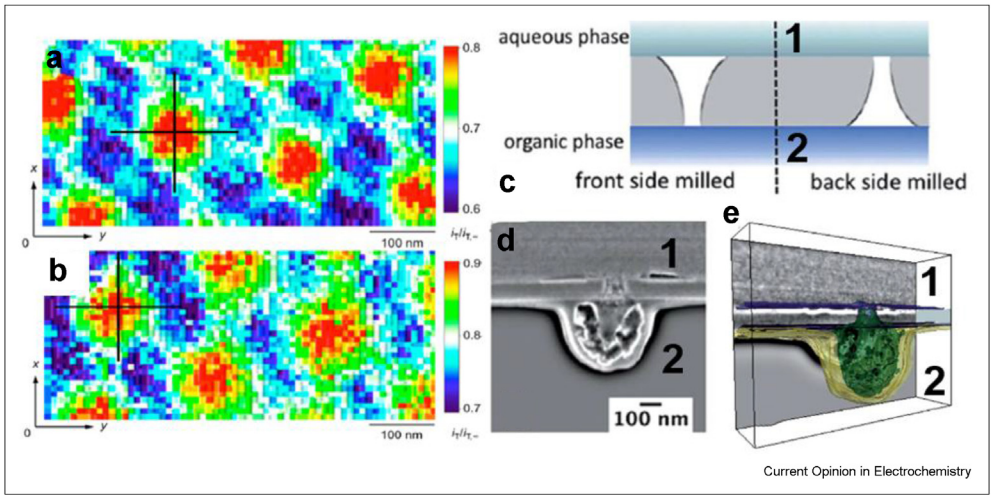

Characterization of the nanopore arrays using ITIES. An SECM image of a Si_3N_4 nanopore array obtained with a non-protruded nanoITIES electrode **(a)** and with a protruded nanoITIES electrode **(b)**. Both SECM images resolved the nanopores in the array. Reprinted with permission from R. Chen, R.J. Balla, A. Lima, S. Amemiya, Characterization of Nanopipet-Supported ITIES Tips for Scanning Electrochemical Microscopy of Single Solid-State Nanopores, Anal. Chem. 89 (2017) 9946−9952. Copyright 2017 American Chemical Society. **(c)** A schematic illustrating the difference between the shape of the front- and back-side milled nanopore arrays as well as their orientations with respect to the ITIES. **(d)** 2D SEM images of a FIB/SEM tomography stack showing the deposit on the nanopore and facing the organic side. **(e)** A 3D reconstruction of the silica deposits generated with a series of images like the one presented in (d). In these figures, the side labeled 1 is the aqueous facing side of the nanopore, while the side labeled 2 is the organic facing side of the nanopore. Adapted from A. Holzinger, G. Neusser, B.J.J. Austen, A. Gamero-Quijano, G. Herzog, D.W.M. Arrigan, A. Ziegler, P. Walther, C. Kranz, Investigation of modified nanopore arrays using FIB/SEM tomography, Faraday Discuss. 210 (2018) 113−130.

DB18C6 and is then detected due to the cationic transfer (Figure 3b) [10]. Electrochemical zwitterionic detection involves numerous equilibrium processes, including the ion-ionophore complexation, acid-base, and partitioning between the oil and aqueous phases equilibria. Later on, Chen, et al. quantitatively studied these equilibria at the nanoITIES [14]. Another study by Chen et al. explored how the tris(crown ether) ionophore TriBCE and mono(crown ether) ionophore DB18C6 differed in the detection of ions using electrochemical methods at the nanoITIES. This study showed that TriBCE enabled easier transfer of ionic species compared to DB18C6 (Figure 3c). This work could provide insights into the molecular design of ionophores for improved sensing of ionic species at the ITIES [13].

Puri and Kim demonstrated another application of the nanoITIES by characterizing the transfer of anionic antimicrobial drugs. These drugs transfer about three orders of magnitude slower from water to DCE than hydrophobic TBA and require more polarized potentials than hydrophobic ClO_4^- to transfer across the water/DCE ITIES (Figure 3d), showing that these ions are 2−5 orders of magnitude more hydrophilic than ClO_4^-. Amperometric detection of these drugs demonstrated the feasibility of using the nanoITIES to identify less hydrophilic drugs that better permeate bacteria [86].

New oil phase solvents for ITIES-based detection have different potential windows than existing solvents, enabling detection of ions that are difficult to detect with existing ITIES systems. Recently, viscous oil phase solvents were shown to have relatively fast ion transfer kinetics at the nanoITIES, allowing for ionic detection across the nanoITIES using these solvents. Chen et al. introduced avocado, coconut, and walnut oils for detecting TBA [40], and Jetmore et al. demonstrated ionic detection with 2-nitrophenyl octyl ether (NPOE) for the first time at the nanoscale, using acetylcholine as the analyte (Figure 3e) [12].

Application of nanoITIES neurotransmitter detection to cellular studies

An exciting application of nanoITIES-based neurotransmitter detection is the ability to perform cellular studies on neurons to better understand their cellular processes, such as exocytosis, synapse formation, and the temporal dependence of neurotransmitter release. Coupling nanoITIES-based detection with SECM enables probing of neuronal processes with enhanced signal-to-noise ratios and detection of real-time spatiotemporal dynamics, etc. SECM enables high spatial resolution probing of neurotransmitter release by positioning a nanoITIES probe within nanometers of a neuronal membrane to detect neurotransmitter flow out of the cell [63,64]. This nanoscale spatial

Figure 3

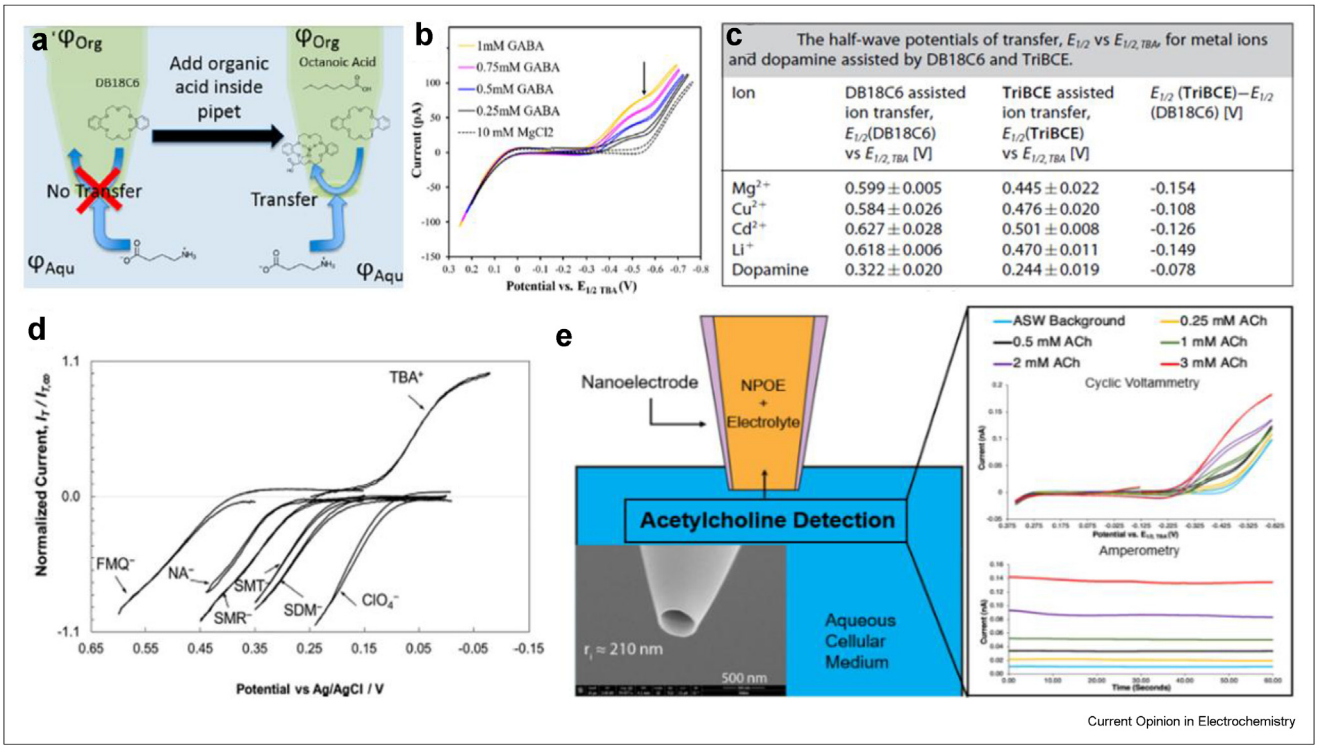

Applications of nanoITIES for neurotransmitter, metal ion detections and biosensing. **(a)** Scheme showing how GABA is detected across the nanoITIES. **(b)** Cyclic voltammetry detection of GABA. Reprinted with permission from N.T. Iwai, M. Kramaric, D. Crabbe, Y. Wei, R. Chen, M. Shen, GABA Detection with Nano-ITIES Pipet Electrode: A New Mechanism, Water/DCE-Octanoic Acid Interface, Anal. Chem. 90 (2018) 3067−3072. Copyright 2018 American Chemical Society. **(c)** Comparison of the transfer potentials of different metal ions and dopamine using two different crown ethers, DB18C6 and TriBCE. Reprinted from R. Chen, A. Yang, A. Chang, P.F. Oweimrin, J. Romero, P. Vichitcharoenpaisarn, S. Tapia, K. Ha, C. Villaflor, M. Shen, A Newly Synthesized Tris(crown ether) Ionophore for Assisted Ion Transfer at NanoITIES Electrodes, ChemElectroChem. 7 (2020) 967−974. **(d)** Voltammograms showing the transfer of antimicrobial drugs at more polarized potentials than the hydrophobic anion. Abbreviations – FMQ: flumequine, NA: nalidixic acid, SMR: sulfamerazine, SMT: sulfamethazine, SDM: sulfadimethoxine, TBA: tetrabutylammonium. Reprinted with permission from S.R. Puri, J. Kim, Kinetics of Antimicrobial Drug Ion Transfer at a Water/Oil Interface Studied by Nanopipet Voltammetry, Anal. Chem. 91 (2019) 1873−1879. Copyright 2019 American Chemical Society. **(e)** Scheme showing how acetylcholine is detected via ion transfer across the nanoITIES, with representative linear detection via cyclic voltammetry and amperometry. Adapted with permission from H.D. Jetmore, C.B. Milton, E.S. Anupriya, R. Chen, K. Xu, M. Shen, Detection of Acetylcholine at Nanoscale NPOE/Water Liquid/Liquid Interface Electrodes, Anal. Chem. 93 (2021) 16535−16542. Copyright 2021 American Chemical Society.

resolution is enabled by the nanoscopic positioning capabilities of SECM [45,47,95,96]. The probe can be placed near neuronal somas or synapses, allowing for studies of neurotransmitter exocytosis from different parts of a neuron. Two studies of neurotransmitter release from neurons of the commonly studied mollusk *Aplysia californica* [97,98] are presented here [63,64].

The first study focused on the somatic exocytosis of acetylcholine from *Aplysia californica* neurons [64]. A nanoITIES electrode was placed ∼140 nm from the soma of an *Aplysia* neuron using an SECM approach (current vs. distance) curve. Chronoamperometry (current vs. time) at the diffusion-limited potential of acetylcholine was used to detect acetylcholine release stimulated by application of high concentration K^+ (Figure 4a) in a selective manner. Numerical simulation of the SECM approach curve determined that the density of releasable vesicles and the cellular permeability to artificial sea water ions were 25 ± 2 vesicles per μm^2 and between 5×10^{-4} and 1×10^{-3} m/s, respectively. The concentration and number of released acetylcholine molecules were measured using amperometry, and further experiments showed that the somatic exocytosis of acetylcholine was Ca^{2+}-dependent. These results demonstrated that nanoITIES electrodes and SECM can effectively characterize neuronal acetylcholine release dynamics with unprecedented high spatiotemporal resolution [64].

The second study focused on the synaptic exocytosis of acetylcholine from *Aplysia californica* neurons [63]. The high spatial resolution of nanoITIES electrodes allows

Figure 4

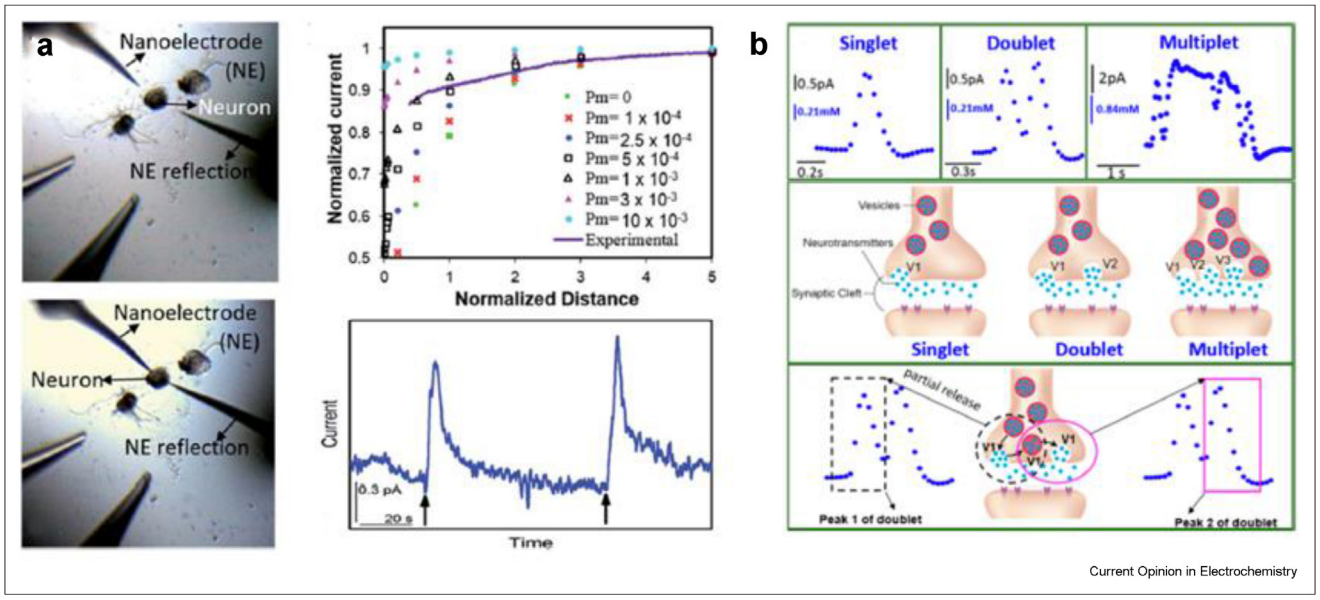

Applications of nanoITIES in cellular studies. **(a)** The detection of acetylcholine release from the soma of *Aplysia californica* neurons after high concentration K^+ stimulation. Data was collected using current–time amperometry at the diffusion-limited potential for acetylcholine. Reprinted from T.M. Welle, K. Alanis, M.L. Colombo, J. V Sweedler, M. Shen, A high spatiotemporal study of somatic exocytosis with scanning electrochemical microscopy and nanoITIES electrodes, Chem. Sci. 9 (2018) 4937–4941. **(b)** The detection of acetylcholine transmission dynamics from the synapse of *Aplysia californica* neurons. The singlet, doublet, and multiplet release mechanisms corresponding to the release of one, two, or more than two vesicles are shown. The occurrence of partial release was also possible. Reprinted with permission from M. Shen, Z. Qu, J. DesLaurier, T.M. Welle, J. V Sweedler, R. Chen, Single Synaptic Observation of Cholinergic Neurotransmission on Living Neurons: Concentration and Dynamics, J. Am. Chem. Soc. 140 (2018) 7764–7768. Copyright 2018 American Chemical Society.

for SECM positioning of the electrode over only the nanoscale synaptic cleft for localized detection of synaptic neurotransmitter release. Acetylcholine release from *Aplysia californica* neuronal synapses was detected after K^+ stimulation using amperometry at the steady-state detection potential of acetylcholine (Figure 4b). This detection revealed release of acetylcholine in singlet, doublet, and multiplet patterns, which were hypothesized to correspond to the release of one, two, or many synaptic vesicles, and a multiple-vesicular-exocytosis mechanism was proposed [63]. A cryogenic electron microscopy study later showed multiple vesicles fusing at one synaptic active zone [99], confirming this hypothesis [63].

Conclusion

We reviewed recent advances in the nanoITIES supported over a nanopipette orifice or a nanopore array during the past five years. These recent advances include nanometer resolution imaging of single nanopores, the introduction of pH modulation strategies to detect neutral species (i.e., zwitterions), probing diffusion profiles (i.e., overlapping vs. independent) in nanopore arrays by performing silica deposition at nanoITIES arrays, characterizing diffusion across a hexagonal nanopore array, and developing new ionophores and viscous oil phases (e.g., avocado oil, coconut oil, NPOE) for analyte sensing. We also discussed applying the nanoITIES as a model of antimicrobial drug transfer across hydrophobic membranes. Finally, we discussed the use of nanoITIES platforms for studying somatic and synaptic exocytosis of neurotransmitters from *Aplysia californica* neurons.

In conclusion, the ITIES has been demonstrated as a versatile analytical platform with the capability to sense metal ions [1–4], proteins [5], neurotransmitters [6–14], in ionic and neutral forms. Detection at the nanoITIES has the analytical advantages of specificity, nanometer spatial resolution [16,56,57], low background current to allow for higher signal-to-noise ratio measurements [16], and high temporal resolution (e.g., millisecond) with chronoamperometry to enable probing fast biological dynamics in real-time. We envision that these new developments and applications will catalyze future research in the interdisciplinary fields of environmental science, ion transfer, electrochemistry, analytical chemistry, biochemistry, and neuroscience.

Declaration of competing interest

The authors declare that they have no known competing financial interests or personal relationships that could have appeared to influence the work reported in this article.

Acknowledgements

This work was funded by a National Science Foundation CAREER Award (CHE 19−45274) to M.S.

References

Papers of particular interest, published within the period of review, have been highlighted as:

* of special interest
** of outstanding interest

1. Evans NJ, Gonsalves M, Gray NJ, Barker AL, Macpherson JV, Unwin PR: **Local amperometric detection of K+ in aqueous solution using scanning electrochemical microscopy ion-transfer voltammetry**. *Electrochem Commun* 2000, **2**:201−206.

2. Zhan D, Li X, Zhan W, Fan F-RF, Bard AJ: **Scanning electrochemical microscopy. 58. Application of a micropipet-supported ITIES tip to detect Ag+ and study its effect on fibroblast cells**. *Anal Chem* 2007, **79**:5225−5231.

3. Stockmann TJ, Montgomery A-M, Ding Z: **Determination of alkali metal ion transfers at liquid|liquid interfaces stabilized by a micropipette**. *J Electroanal Chem* 2012, **684**:6−12.

4. Nestor U, Wen H, Girma G, Mei Z, Fei W, Yang Y, Zhang C, Zhan D: **Facilitated Li+ ion transfer across the water/1,2-dichloroethane interface by the solvation effect**. *Chem Commun* 2014, **50**:1015−1017.

5. Arrigan DWM, Hackett MJ, Mancera RL: **Electrochemistry of proteins at the interface between two immiscible electrolyte solutions**. *Curr Opin Electrochem* 2018, **12**:27−32.

6. Zhan D, Mao S, Zhao Q, Chen Z, Hu H, Jing P, Zhang M, Zhu Z, Shao Y: **Electrochemical investigation of dopamine at the water/1,2-dichloroethane interface**. *Anal Chem* 2004, **76**:4128−4136.

7. Shao Y, Girault HH: **Kinetics of the transfer of acetylcholine across the water + sucrose/1,2-dichloroethane interface: a comparison between ion transport and ion transfer**. *J Electroanal Chem Interfacial Electrochem* 1990, **282**:59−72.

8. Colombo ML, McNeil S, Iwai N, Chang A, Shen M: **Electrochemical detection of dopamine via assisted ion transfer at nanopipet electrode using cyclic voltammetry**. *J Electrochem Soc* 2015, **163**:H3072−H3076.

9. Colombo ML, Sweedler JV, Shen M: **Nanopipet-based liquid-liquid interface probes for the electrochemical detection of acetylcholine, tryptamine, and serotonin via ionic transfer**. *Anal Chem* 2015, **87**:5095−5100.

10. ** Iwai NT, Kramaric M, Crabbe D, Wei Y, Chen R, Shen M: **GABA detection with nano-ITIES Pipet electrode: a new mechanism, water/DCE-octanoic acid interface**. *Anal Chem* 2018, **90**:3067−3072.
This paper demonstrates the ability to use the ITIES for detecting neutral zwitterions by introducing a strategy based on pH modulation. This capability expands the applicability of the ITIES to cellular studies for detecting neutral biomolecules, such as many proteins and some neurotransmitters.

11. Beni V, Ghita M, Arrigan DWM: **Cyclic and pulse voltammetric study of dopamine at the interface between two immiscible electrolyte solutions**. *Biosens Bioelectron* 2005, **20**:2097−2103.

12. * Jetmore HD, Milton CB, Anupriya ES, Chen R, Xu K, Shen M: **Detection of acetylcholine at nanoscale NPOE/water liquid/liquid interface electrodes**. *Anal Chem* 2021, **93**:16535−16542.
This paper demonstrates use of 2-nitrophenyl octyl ether as a new, viscous ITIES solvent for the first time at the nanoscale ITIES for in vitro sensing, laying the foundation for future cellular studies. This solvent's distinct potential window from existing nanoITIES solvents could allow for easier detection of certain analytes.

13. Chen R, Yang A, Chang A, Oweimrin PF, Romero J, Vichitcharoenpaisarn P, Tapia S, Ha K, Villaflor C, Shen M: **A newly synthesized tris(crown ether) ionophore for assisted ion transfer at NanoITIES electrodes**. *Chemelectrochem* 2020, **7**:967−974.

14. Chen R, McAllister AB, Shen M: **Detection of zwitterion at an electrified liquid-liquid interface: a chemical equilibrium perspective**. *J Electroanal Chem* 2020, **873**:114303.

15. Samec Z: **Electrochemistry at the interface between two immiscible electrolyte solutions (IUPAC Technical Report)**. *Pure Appl Chem* 2004, **76**:2147−2180.

16. Shen M, Colombo ML: **Electrochemical nanoprobes for the chemical detection of neurotransmitters**. *Anal Methods* 2015, **7**:7095−7105.

17. Shen M, Chen R: **Real time studies of acetylcholine release from single synapses and single cells with nanometer spatial resolution**. In *Compend. Vivo monit. Real-time mol. Neurosci. Vol. Probing brain funct. Dis. Inj. With enhanc. Opt. Electrochem. Sensors, NV-1 onl.* Edited by Wilson GS, Michael AC, Singapore: World Scientific Publishing Co. Pte. Ltd.; 2020.

18. Cabana J, Alaan T, Crabtree GW, Hatzell MC, Manthiram K, Steingart DA, Zenyuk I, Jiao F, Vojvodic A, Yang JY, Balsara NP, Persson KA, Siegel DJ, Haynes CL, Mauzeroll J, Shen M, Venton BJ, Balke N, Rodríguez-López J, Rolison DR, Shahbazian-Yassar R, Srinivasan V, Chaudhuri S, Couet A, Hattrick-Simpers J, NGenE: **Electrochemistry is everywhere**. *ACS Energy Lett n.d.* 2021:368−374. 0.

19. Arrigan DWM, Ghita M, Beni V: **Selective voltammetric detection of dopamine in the presence of ascorbate**. *Chem Commun* 2004:732−733.

20. Herzog G, McMahon B, Lefoix M, Mullins ND, Collins CJ, Moynihan HA, Arrigan DWM: **Electrochemistry of dopamine at the polarised liquid|liquid interface facilitated by an homo-oxo-calix[3]arene ionophore**. *J Electroanal Chem* 2008, **622**:109−114.

21. Tatsumi H, Ueda T: **Ion transfer voltammetry of tryptamine, serotonin, and tryptophan at the nitrobenzene/water interface**. *J Electroanal Chem* 2011, **655**:180−183.

22. Marcus RA: **On the theory of ion transfer rates across the interface of two immiscible liquids**. *J Chem Phys* 2000, **113**:1618−1629.

23. Ballantyne AD, Brisdon AK, Dryfe RAW: **Immiscible electrolyte systems based on asymmetric hydrophobic room temperature ionic liquids**. *Chem Commun* 2008:4980−4982.

24. Silvester DS, Arrigan DWM: **Array of water|room temperature ionic liquid micro-interfaces**. *Electrochem Commun* 2011, **13**:477−479.

25. Wang E, Sun Z: **Ion transfer of Bromocresol Green across liquid-liquid interfaces**. *Anal Chem* 1987, **59**:1414−1417.

26. Wang Y, Kakiuchi T, Yasui Y, Mirkin MV: **Kinetics of ion transfer at the ionic liquid/water nanointerface**. *J Am Chem Soc* 2010, **132**:16945−16952.

27. Jing P, Zhang M, Hu H, Xu X, Liang Z, Li B, Shen L, Xie S, Pereira CM, Shao Y: **Ion-transfer reactions at the nanoscopic water/n-octanol interface**. *Angew Chem Int Ed* 2006, **45**:6861−6864.

28. Sun P, Laforge FO, Mirkin MV: **Ion transfer at nanointerfaces between water and neat organic solvents**. *J Am Chem Soc* 2005, **127**:8596−8597.

29. Alanis K, Alden SE, Baker LA, Satheesan AE, Jetmore HD, Shen M: **Micro and nanopipettes for electrochemical imaging and measurement**. In *Scanning Electrochemical Microscopy*. Edited by Bard AJ, Mirkin MV. 3rd ed. 2022.

30. Gu C, Nie X, Jiang J, Chen Z, Dong Y, Zhang X, Liu J, Yu Z, Zhu Z, Liu J, Liu X, Shao Y: **Mechanistic study of oxygen reduction at liquid/liquid interfaces by hybrid ultra-microelectrodes and mass spectrometry**. *J Am Chem Soc* 2019, **141**:13212−13221.

31. Shao Y. In *Electrochemistry at liquid/liquid interfaces*. Edited by T.-H CGB, Zoski of E, Amsterdam: Elsevier; 2007:785−809.

32. Girault HH: **Electrochemistry at the interface between two immiscible electrolyte solutions**. *Electrochim Acta* 1987, **32**:383−385.

33. Senda M, Kakiuchi T, Osaka T: **Electrochemistry at the interface between two immiscible electrolyte solutions**. *Electrochim Acta* 1991, **36**:253–262.

34. Liu B, Mirkin MV: **Electrochemistry at microscopic liquid–liquid interfaces**. *Electroanalysis* 2000, **12**:1433–1446.

35. Amemiya S, Wang Y, Mirkin MV: **Nanoelectrochemistry at the liquid/liquid interfaces**. In Compton RG, Wadhawan JD. *Electrochem*, vol. 12. Cambridge, UK: Nanoelectrochemistry, The Royal Society of Chemistry; 2013:1–43.

36. Arrigan DWM, Herzog G: **Theory of electrochemistry at miniaturised interfaces between two immiscible electrolyte solutions**. *Curr Opin Electrochem* 2017, **1**:66–72.

37. Li Q, Xie S, Liang Z, Meng X, Liu S, Girault HH, Shao Y: **Fast ion-transfer processes at nanoscopic liquid/liquid interfaces**. *Angew Chem Int Ed* 2009, **48**:8010–8013.

38. Sun Z, Wang E: **Some solvents and supporting electrolytes studied for electrochemical measurement at liquid/liquid interface**. *Electroanalysis* 1989, **1**:507–515.

39. Stockmann TJ, Ding Z: **Hydrophobicity of room temperature ionic liquids assessed by the Galvani potential difference established at micro liquid/liquid interfaces**. *J Electroanal Chem* 2010, **649**:23–31.

40. Chen R, Xu K, Shen M: **Avocado oil, coconut oil, walnut oil as true oil phase for ion transfer at nanoscale liquid/liquid interfaces**. *Electrochim Acta* 2020, **357**:136788.

41. Shao Y, Mirkin M V: Voltammetry at micropipet electrodes. Anal Chem n.d., 70: 3155–3161.

42. Ulmeanu SM, Jensen H, Samec Z, Bouchard G, Carrupt P-A, Girault HH: **Cyclic voltammetry of highly hydrophilic ions at a supported liquid membrane**. *J Electroanal Chem* 2002, **530**:10–15.

43. Ulmeanu SM, Jensen H, Bouchard G, Carrupt P-A, Girault HH: **Water-oil partition profiling of ionized drug molecules using cyclic voltammetry and a 96-well microfilter plate system**. *Pharm Res (N Y)* 2003, **20**:1317–1322.

44. Nishi N, Kawakami T, Shigematsu F, Yamamoto M, Kakiuchi T: **Fluorine-free and hydrophobic room-temperature ionic liquids, tetraalkylammonium bis(2-ethylhexyl)sulfosuccinates, and their ionic liquid–water two-phase properties**. *Green Chem* 2006, **8**:349–355.

45. Mirkin MV, Amemiya S. In *Nanoelectrochemistry*. 1st ed. Boca Raton: CRC Press/Taylor and Francis Group; 2015.

46. Kim J, Shen M, Nioradze N, Amemiya S: **Stabilizing nanometer scale tip-to-substrate gaps in scanning electrochemical microscopy using an isothermal chamber for thermal drift suppression**. *Anal Chem* 2012, **84**:3489–3492.

47. Shen M, Ishimatsu R, Kim J, Amemiya S: **Quantitative imaging of ion transport through single nanopores by high-resolution scanning electrochemical microscopy**. *J Am Chem Soc* 2012, **134**:9856–9859.

48. Rodgers PJ, Amemiya S, Wang Y, Mirkin MV: **Nanopipet voltammetry of common ions across the Liquid–Liquid interface. Theory and limitations in kinetic analysis of nanoelectrode Voltammograms**. *Anal Chem* 2010, **82**:84–90.

49. Mareček V, Samec Z, Koryta J: **Charge transfer across the interface of two immiscible electrolyte solutions**. *Adv Colloid Interface Sci* 1988, **29**:1–78.

50. Vanysek P, Buck RP: **New development in liquid/liquid interface transport. A literature review**. *J Electroanal Chem Interfacial Electrochem* 1984, **163**:1–9.

51. Izadyar A: **Stripping voltammetry at the interface between two immiscible electrolyte solutions: a review paper**. *Electroanalysis* 2018, **30**:2210–2221.

52. Terry Weatherly CK, Ren H, Edwards MA, Wang L, White HS: **Coupled electron- and phase-transfer reactions at a three-phase interface**. *J Am Chem Soc* 2019, **141**:18091–18098.

53. Rastgar S, Pilarski M, Wittstock G: **A polarized liquid–liquid interface meets visible light-driven catalytic water oxidation**. *Chem Commun* 2016, **52**:11382–11385.

54. Amemiya S, Ding Z, Zhou J, Bard AJ: **Studies of charge transfer at liquid|liquid interfaces and bilayer lipid membranes by scanning electrochemical microscopy**. *J Electroanal Chem* 2000, **483**:7–17.

55. Samec Z, Mareček V, Koryta J, Khalil MW: **Investigation of ion transfer across the interface between two immiscible electrolyte solutions by cyclic voltammetry**. *J Electroanal Chem Interfacial Electrochem* 1977, **83**:393–397.

56. Sun T, Yu Y, Zacher BJ, Mirkin MV: **Scanning electrochemical microscopy of individual catalytic nanoparticles**. *Angew Chem Int Ed* 2014, **53**:14120–14123.

57. Chen Q, Luo L, Faraji H, Feldberg SW, White HS: **Electrochemical measurements of single H2 nanobubble nucleation and stability at Pt nanoelectrodes**. *J Phys Chem Lett* 2014, **5**:3539–3544.

58. Nioradze N, Chen R, Kim J, Shen M, Santhosh P, Amemiya S: **Origins of nanoscale damage to glass-sealed platinum electrodes with submicrometer and nanometer size**. *Anal Chem* 2013, **85**:6198–6202.

59. ** Holzinger A, Neusser G, Austen BJJ, Gamero-Quijano A, Herzog G, Arrigan DWM, Ziegler A, Walther P, Kranz C: **Investigation of modified nanopore arrays using FIB/SEM tomography**. *Faraday Discuss* 2018, **210**:113–130.
This paper demonstrates the potential of FIB/SEM tomography for investigating nanopore arrays with the aim of localizing the interface between two immiscible electrolyte solutions via the visualization of electrochemically deposited silica at nanoporous arrays.

60. Liu Y, Holzinger A, Knittel P, Poltorak L, Gamero-Quijano A, Rickard WDA, Walcarius A, Herzog G, Kranz C, Arrigan DWM: **Visualization of diffusion within nanoarrays**. *Anal Chem* 2016, **88**:6689–6695.

61. ** Chen R, Balla RJ, Lima A, Amemiya S: **Characterization of nanopipet-supported ITIES tips for scanning electrochemical microscopy of single solid-state nanopores**. *Anal Chem* 2017, **89**:9946–9952.
This is a second paper following previous one in 2012 (JACS, 2012, 134, 9856–9859) in nanometer-resolution imaging of nanopores achieved with nanoITIES and SECM. This work imaged nanopore arrays using protruded nanoITIES, where each nanopore has been clearly resolved with nanometer resolution, showing that protruded interfaces at nanoITIES tips does not compromise spatial resolution for imaging.

62. * Liu Y, Moshrefi R, Rickard WDA, Scanlon MD, Stockmann TJ, Arrigan DWM: **Ion-transfer electrochemistry at arrays of nanoscale interfaces between two immiscible electrolyte solutions arranged in hexagonal format**. *J Electroanal Chem* 2022, **909**:116113.
This paper characterizes a new nanopore array geometry, namely a hexagonal arrangement of nanopores that has the benefit of constant spacing between nanopores so that the diffusion mode across each pore is identical. The required ratio of center-to-center distance between nanopores and radius of the nanopores needed to be at least 96 to allow for independent diffusion across the nanopores, which was larger than the required ratio for independent diffusion across square nanopore arrays.

63. ** Shen M, Qu Z, DesLaurier J, Welle TM, Sweedler JV, Chen R: **Single synaptic observation of cholinergic neurotransmission on living neurons: concentration and dynamics**. *J Am Chem Soc* 2018, **140**:7764–7768.
This paper pioneered in interrogating acetylcholine exocytosis at synapses of in vitro *Aplysia californica* neurons using the nanoITIES. Singlet, doublet, and multiplet release patterns were hypothesized to correspond to one, two, or many vesicles undergoing simultaneous exocytosis, respectively, and a multi-vesicular-exocytosis mechanism was introduced.

64. * Welle TM, Alanis K, Colombo ML, Sweedler JV, Shen M: **A high spatiotemporal study of somatic exocytosis with scanning electrochemical microscopy and nanoITIES electrodes**. *Chem Sci* 2018, **9**:4937–4941.

This paper detected the release of acetylcholine from the soma of *Aplysia californica* neurons and quantified the neuronal membrane's permeability and the density of releasable vesicles. This study also established the calcium dependence of acetylcholine somatic exocytosis.

65. Mareček V, Samec Z: **Ion transfer kinetics at the interface between two immiscible electrolyte solutions supported on a thick-wall micro-capillary. A mini review**. *Curr Opin Electrochem* 2017, **1**:133–139.

66. Bard AJ, Faulkner LR: *Electrochemical methods: fundamentals and applications*. New York: Wiley; 2001.

67. Reymond F, Carrupt P-A, Girault HH: **Facilitated ion transfer reactions across oil|water interfaces. Part I. Algebraic development and calculation of cyclic voltammetry experiments for successive complex formation**. *J Electroanal Chem* 1998, **449**:49–65.

68. Girault HH: **Electrochemistry at liquid–liquid interfaces**. In Bard AJ, Zoski CG, vol. 23. Boca Raton: CRC Press; 2010:1–104.

69. Lefrou C: **A unified new analytical approximation for positive feedback currents with a microdisk SECM tip**. *J Electroanal Chem* 2006, **592**:103–112.

70. Su B, Eugster N, Girault HH: **Simulations of the adsorption of ionic species at polarisable liquid|liquid interfaces**. *J Electroanal Chem* 2005, **577**:187–196.

71. Pereira CM, Schmickler W, Silva F, Sousa MJ: **Ion association at liquid|liquid interfaces**. *J Electroanal Chem* 1997, **436**:9–15.

72. Trojánek A, Lhotský A, Mareček V, Samec Z: **Limited agreement between the interfacial tension and differential capacity data for the polarised water|1,2-dichloroethane interface**. *J Electroanal Chem* 2004, **565**:243–250.

73. Guangming L, Sarka M, Jaesung Y, G SD, Binhua L, Mati M, Ilan B, Petr V, Sm L: **Ion distributions near a liquid-liquid interface**. *Science* 2006, **311**:216–218. 80-.

74. Nouamane L, Miroslav M, Binyang H, Hao Y, Petr V, Mati M, Binhua L, Ilan B, Sm L: **Tuning ion correlations at an electrified soft interface**. *Proc Natl Acad Sci Unit States Am* 2012, **109**:20326–20331.

75. Dl B, Yuki N, Helmut L, Grazia G, Johannes H, Beh G: **Mischa B: saturation of charge-induced water alignment at model membrane surfaces**. *Sci Adv* 2022, **4**:eaap7415.

76. Tummino A, Scoppola E, Fragneto G, Gutfreund P, Maestro A, Dryfe RAW: **Neutron reflectometry study of the interface between two immiscible electrolyte solutions: effects of electrolyte concentration, applied electric field, and lipid adsorption**. *Electrochim Acta* 2021, **384**:138336.

77. Trojánek A, Mareček V, Samec Z: **Mixed electrolyte effect on the stability of the interface between two immiscible electrolyte solutions**. *Electrochim Acta* 2021, **399**:139405.

78. ** Gschwend GC, Olaya A, Girault HH: **How to polarise an interface with ions: the discrete Helmholtz model**. *Chem Sci* 2020, **11**:10807–10813.
This work showed that ITIES is devoid of diffuse layer. The lack of a diffuse layer results from the ions interacting across short distances at the ITIES. They also concluded that models based on the Poisson–Boltzmann equation do not satisfactorily describe ion distributions at polarized liquid–liquid interfaces as evidenced by the findings from this work.

79. Trojánek A, Mareček V, Samec Z: **Capacitance of the interface between two immiscible electrolyte solutions – a controversial issue**. *Electrochim Acta* 2022, **403**:139720.

80. Verwey EJW, Niessen KF: **XL. The electrical double layer at the interface of two liquids. London, Edinburgh**. *Dublin Philos Mag J Sci* 1939, **28**:435–446.

81. Verwey EJW: **Electrical double layer and stability of emulsions**. *Trans Faraday Soc* 1940, **35**:192–203.

82. Cai C, Mirkin MV: **Electron transfer kinetics at polarized nanoscopic liquid/liquid interfaces**. *J Am Chem Soc* 2006, **128**:171–179.

83. Shao Y, Mirkin MV: **Fast kinetic measurements with nanometer-sized pipets. Transfer of potassium ion from water into dichloroethane facilitated by dibenzo-18-crown-6**. *J Am Chem Soc* 1997, **119**:8103–8104.

84. Zhang S, Li M, Su B, Shao Y: **Fabrication and use of nanopipettes in chemical analysis**. *Annu Rev Anal Chem* 2018, **11**:265–286.

85. Yu R-J, Ying Y-L, Gao R, Long Y-T: **Confined nanopipette sensing: from single molecules, single nanoparticles, to single cells**. *Angew Chem Int Ed* 2019, **58**:3706–3714.

86. ** Puri SR, Kim J: **Kinetics of antimicrobial drug ion transfer at a water/oil interface studied by nanopipet voltammetry**. *Anal Chem* 2019, **91**:1873–1879.
This paper modeled the hydrophobic bacterial cell membrane using the DCE/water nanoITIES. Hydrophilic antimicrobial drug ions transferred slower than hydrophobic cations and anions, suggesting that antimicrobial drugs with more hydrophobic characteristics could evade bacterial resistance.

87. Zhou M, Yu Y, Blanchard P-Y, Mirkin MV: **Surface patterning using Diazonium Ink filled nanopipette**. *Anal Chem* 2015, **87**:10956–10962.

88. Alden SE, Siepser NP, Patterson JA, Jagdale GS, Choi M, Baker LA: **Array microcell method (AMCM) for serial electroanalysis**. *Chemelectrochem* 2020, **7**:1084–1091.

89. Shigyou K, Sun L, Yajima R, Takigaura S, Tajima M, Furusho H, Kikuchi Y, Miyazawa K, Fukuma T, Taoka A, Ando T, Watanabe S: **Geometrical characterization of glass nanopipettes with sub-10 nm pore diameter by transmission electron microscopy**. *Anal Chem* 2020, **92**:15388–15393.

90. Sa N, Baker LA: **Experiment and simulation of ion transport through nanopipettes of well-defined conical geometry**. *J Electrochem Soc* 2013, **160**:H376–H381.

91. Amemiya S, Kim J, Izadyar A, Kabagambe B, Shen M, Ishimatsu R: **Electrochemical sensing and imaging based on ion transfer at liquid/liquid interfaces**. *Electrochim Acta* 2013, **110**:836–845.

92. Perry D, Momotenko D, Lazenby RA, Kang M, Unwin PR: **Characterization of nanopipettes**. *Anal Chem* 2016, **88**:5523–5530.

93. Morris CA, Friedman AK, Baker LA: **Applications of nanopipettes in the analytical sciences**. *Analyst* 2010, **135**:2190–2202.

94. Sun P, Mirkin MV: **Scanning electrochemical microscopy with slightly recessed nanotips**. *Anal Chem* 2007, **79**:5809–5816.

95. Bard AJ, Mirkin MV. *Scanning electrochemical microscopy*. New York: Marcel Dekker; 2001.

96. Amemiya S, Bard AJ, Fan F-RF, Mirkin MV, Unwin PR: **Scanning electrochemical microscopy**. *Annu Rev Anal Chem* 2008, **1**:95–131.

97. Moroz LL: **Aplysia**. *Curr Biol* 2011, **21**:R60–R61.

98. Walters ET, Carew TJ, Kandel ER: **Associative learning in Aplysia: evidence for conditioned fear in an invertebrate**. *Science* 1981, **211**:504–506. 80-.

99. Kusick GF, Chin M, Raychaudhuri S, Lippmann K, Adula KP, Hujber EJ, Vu T, Davis MW, Jorgensen EM, Watanabe S: **Synaptic vesicles transiently dock to refill release sites**. *Nat Neurosci* 2020, **23**:1329–1338.